Journal of Alloys and Compounds 507 (2010) 261–266

Contents lists available at ScienceDirect

Journal of Alloys and Compounds

journal homepage: www.elsevier.com/locate/jallcom

Density- and adhesion-controlled ZnO nanorod arrays on the ITO flexible substrates and their electrochromic performance

Anzheng Hu[a,b], Fei Wu[a], Jinping Liu[a], Jian Jiang[a], Ruimin Ding[a], Xin Li[a], Cuixia Cheng[a], Zhihong Zhu[a], Xintang Huang[a,*]

[a] Institute of Nanoscience and Nanotechnology, Central China Normal University, Wuhan 430079, PR China
[b] School of Physics and Electronic Engineering, Xiangfan University, Xiangfan 441053, Hubei, PR China

ARTICLE INFO

Article history:
Received 16 March 2010
Received in revised form 22 July 2010
Accepted 28 July 2010
Available online 4 August 2010

Keywords:
ZnO nanorod arrays
Density- and adhesion-controlled
Flexible substrate
Electrochromic performance

ABSTRACT

We report large-scale density- and adhesion-controlled ZnO nanorod arrays (NRs) directly grown on flexible ITO/PET substrates and have studied their absorption capability to viologen molecules and electrochromic performance. The density can be readily controlled by adjusting the thickness of pre-prepared ZnO seed layers. And the adhesion property of the ZnO NRs to substrates can be controlled by different methods of pre-preparation ZnO seed layer. The effect indicates that the ZnO NRs using sputtering-prepared seed layers show superior adhesion property to substrate and resistance capacity to ultrasonicating and bending when compared with the spin-coated method. Moreover, it has been found that the ZnO NRs, with optimum density and occupied space ratio (OSR) (density, ~3.34×10^9 rods cm^{-2}; diameter, ~140 nm; and OSR, ~52%), demonstrate optimal absorption capability to viologen molecules and excellent electrochromic performance.

1. Introduction

ZnO nanorod arrays (NRs), as an excellent member in the family of one-dimensional (1D) nanostructures, have been received increased attention because of their excellent electrical and optical properties. Moreover, it has been found that spectacular applications in fabricating electronic, optoelectronic, electrochemical, and electromechanical devices such as ultraviolet (UV) lasers [1], light-emitting diodes [2], field-emission devices [3–6], field effect transistors, transparent conductors [7], solar cells [8] and piezo-nanogenerators [9,10], especially in the field of electrochromic devices (ECs) [11] including flexible and transparent ECs, have also showed considerable merit owing to reversibly changing their optical properties upon charge injection and extraction induced by the external voltage. Due to the ECs' quick response time and great repeatability, low operation voltage and energy consumption, high coloration efficiency and rich color availability, flexible substrate and large scale but lightness of weight, and long open circuit memory effects, enabled them to possess many potential applications including electrochromic (EC) displays, smart windows, electropapers and electrobillboards [11–14].

It is well known that one-dimensional ZnO nanostructure materials (e.g., ZnO NRs) are excellent working electrodes of the ECs made of one working electrode, one counter electrode, and one ion conductive layer in between because of their large surface area [11], high crystallization performance and good electron transport properties. Furthermore, ZnO, as a nontoxic n-type semiconductor (Eg = 3.37 eV), is even more attractive for high-efficiency short wavelength optoelectronic nanodevices on account of its large exciton binding energy of 60 meV and high mechanical and thermal stabilities. On the other hand, ZnO is a wide band gap II–VI semiconductor and a cheap and nontoxic material. Utilization of ZnO in ECs may further reduce the cost. However, there are few reports on the fabrication of density- and adhesion-controlled ZnO NRs on flexible ITO/PET (indium tin oxide/polyethylene terephthalate) transparent substrate (IPS), though lots of papers have focused on fabrication of ZnO nanostructures [6,15–18].

In this communication, we embarked on for the first time a study that the large-scale ZnO NRs were grown directly on flexible IPS, especially more attention was paid to investigate the density, occupied space ratio (OSR) and adhesion property to the substrate of ZnO NRs. Meanwhile, relevant kinetics conditions of NRs growth were discussed as well, including concentrations and ratios of the starting reactants, such as zinc nitrate hexahydrate ($Zn(NO_3)_2{\cdot}6H_2O$) to hexamethylenetetramine ($C_6H_{12}N_4$), and including the growth temperature and time. And then, EC performance study was divided into two steps, modifying methyl viologen and exploring EC performance using three electrodes sys-

* Corresponding author. Fax: +86 27 67861185.
E-mail addresses: sporthaz@126.com (A. Hu), xthuang@phy.ccnu.edu.cn (X. Huang).

0925-8388/$ – see front matter © 2010 Elsevier B.V. All rights reserved.
doi:10.1016/j.jallcom.2010.07.173

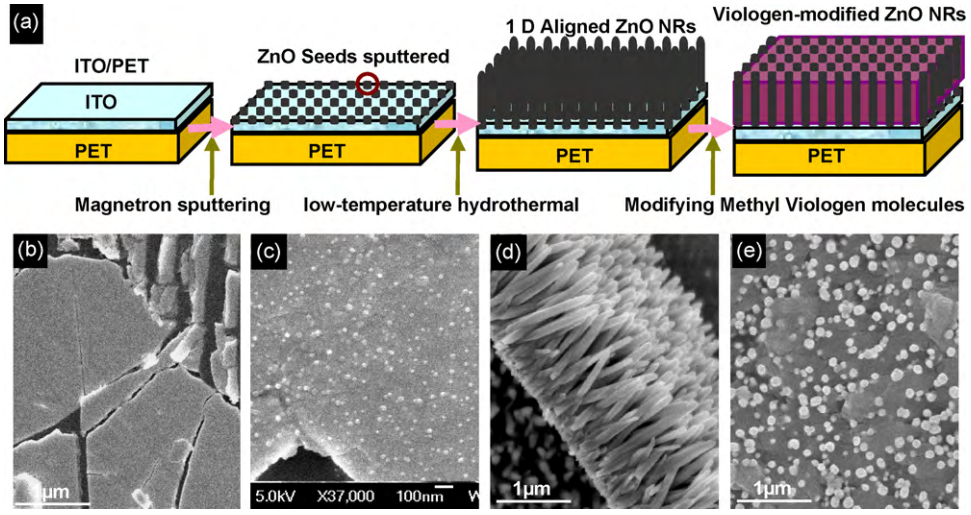

Fig. 1. (a) The schematic approach of growing ZnO NRs on IPS and modifying with viologen molecules, (b) before and (c) after sputtering ZnO seed layers on the original IPS, (d) the image after growth 1D vertically aligned ZnO NRs on (c), and (e) the image after (d) modified methyl viologen molecules.

tem. SEM, TEM and XRD were also employed to characterize the ZnO NRs.

The novel ZnO NRs grown on IPS have at least three advantages. First, it provides a way to fabricate vertically aligned ZnO arrays on flexible IPS. Second, the flexible substrates could be easily designed into various sizes and shapes, and thus providing tremendous flexibility for ZnO NRs' applications. Third, these unique advantages make ZnO nanorods a promising matrix electrode for EC dye molecule loading.

2. Experimental

All chemicals (from Shanghai Chemicals Co. Ltd.) used in this work were of analytical reagent grade and used as received without further treatments.

2.1. Preparation process

The viologen-modified ZnO NRs (VMZs) EC working electrodes were achieved by three main steps. The first step was that a thin layer of ZnO film, about 4–5 nm thickness, was deposited on the IPS as seed using spin-coating or sputter-coating method [11] before the growth of ZnO NRs. The coating solution was obtained by mixing 0.03 M NaOH solution of ethanol and 0.01 M zinc acetate dehydrate ($Zn(CH_3COO)_2{\cdot}2H_2O$) solution of ethanol, the volume ratio is 1–3, and then the coating solution was spin-coated onto IPS at 500 rpm for several times according to the expected thickness of ZnO seed layer [19], and between every two layers, the seeded IPS was subsequently baked for about 15 min in oven at 50 °C. With regard to magnetron sputtering method, the ZnO seed layer was readily obtained by FJL560 magnetron sputtering equipment, and which was deposited at a distance of 57 mm between target and IPS, a base vacuum of 5×10^{-4} Pa, a sputtering power of ~55 W, an argon pressure of 0.5 Pa and ~80 s sputtering time. Different density ZnO NRs were obtained mainly by adjusting the sputtering time. The second step was the growth of, as we know, the ZnO nanostructure array was hydrothermally prepared using the procedures reported elsewhere [6,20–22]. In our work, the seeded IPSs obtained from the first step were suspended in 300 mL of aqueous solutions containing 0.05 M $Zn(NO_3)_2{\cdot}6H_2O$ and 0.06 M $C_6H_{12}N_4$ in a sealed beaker [23] following by heating at a temperature of 75 °C for 24 h. Changing the molar ratio of reactants, the growth temperature and time resulted in the formation of 1D ZnO NRs with different densities and OSRs. Slight stirring was maintained throughout the entire process. After the reaction, these substrates covered tightly with ZnO nanostructures were rinsed with ethanol and dried in air for further characterization. Finally, the as-grown ZnO NRs of different densities and OSRs were first treated by oxygen plasma for 5 min and baked in an oven at 60 °C for 1 h. Then these arrays were immersed in a 0.02 M aqueous solutions of methyl viologen at 40 °C for 72 h, followed by a wash with 2-propanol to remove the unattached viologen. Subsequently, the VMZs electrodes were dried in air and stored in a vacuumed dark chamber for 24 h prior to use.

2.2. EC performance

The VMZs of different OSRs were assembled as working electrodes of the three electrodes system and immersed in an electrolyte containing 0.2 M $LiClO_4$ γ-butyrolactone solution. Then the EC photographs and EC current potential (CV) curves of the various electrodes were obtained for further research. It is worth pointing out that all the chemical materials and the electrolytes were bubbled with dry N_2 prior to the experiment since the performance of the EC is sensitive to oxygen.

2.3. Characterization

The morphology, size and property of the products were characterized by field-emission scanning electron microscopy (FESEM, JEOL, JSM-6700F), and the identity and the phase were analyzed using an X-ray diffractometer (XRD, Cu Kα radiation; λ = 1.5418 Å) at a scan rate of 0.06 s^{-1}. The selected area electron diffraction (SAED) pattern, transmission electron microscopy (TEM) and high-resolution transmission electron microscopy (HRTEM) observations of the products were all carried out on a JEOL JEM-2010 instrument. The cyclic voltammograms (CVs) of the ZnO nanowire electrode were recorded by a CHI660C electrochemical instrument, and the test was carried out in a standard three electrodes system (vs Ag/AgCl sat. KCl reference electrode).

3. Results and discussion

3.1. Schematic approach and images of EC working electrode

Herein, the formation mechanism of the VMZs is schematically illustrated in Part a of Fig. 1 and its corresponding FESEM images in Parts b–e of Fig. 1 (some big cracks in Fig. 1b and c made for the comparison with their substrates). Part b of Fig. 1 shows the bare IPS. Through the pre-sputtering process on Part b, a thin layer ZnO seed made of little crystalline nanoparticles with a diameter of 10–20 nm was coated on the IPS, as shown in Part c of Fig. 1. And then, Part d of Fig. 1 shows the ZnO NRs grown using a low-temperature hydrothermal decomposition method. Finally, the VMZs used as EC working electrode is shown in Part e of Fig. 1.

3.2. Morphology and microstructure

The top-view and cross-sectional scanning electron microscopy (SEM) images of the as-prepared ZnO NRs on IPS can be clearly shown in Fig. 2 (Fig. 2a, the low-magnification; Fig. 2b, the relatively high-magnification with two inserts: the regular cross-section and magnificent enhanced images). ZnO NRs is characterized by large-area hexagonal ZnO nanorod arrays with uniform growth density, and it was obtained by using the mixing solution of 0.05 M $Zn(NO_3)_2{\cdot}6H_2O$ and 0.06 M $C_6H_{12}N_4$ at 75 °C for 24 h.

XRD patterns of the above-mentioned ZnO NRs are summarized in Fig. 2c. The strongest peaks are (0 0 2), indicating that individual ZnO nanostructures and crystallized along the *c*-axis direction

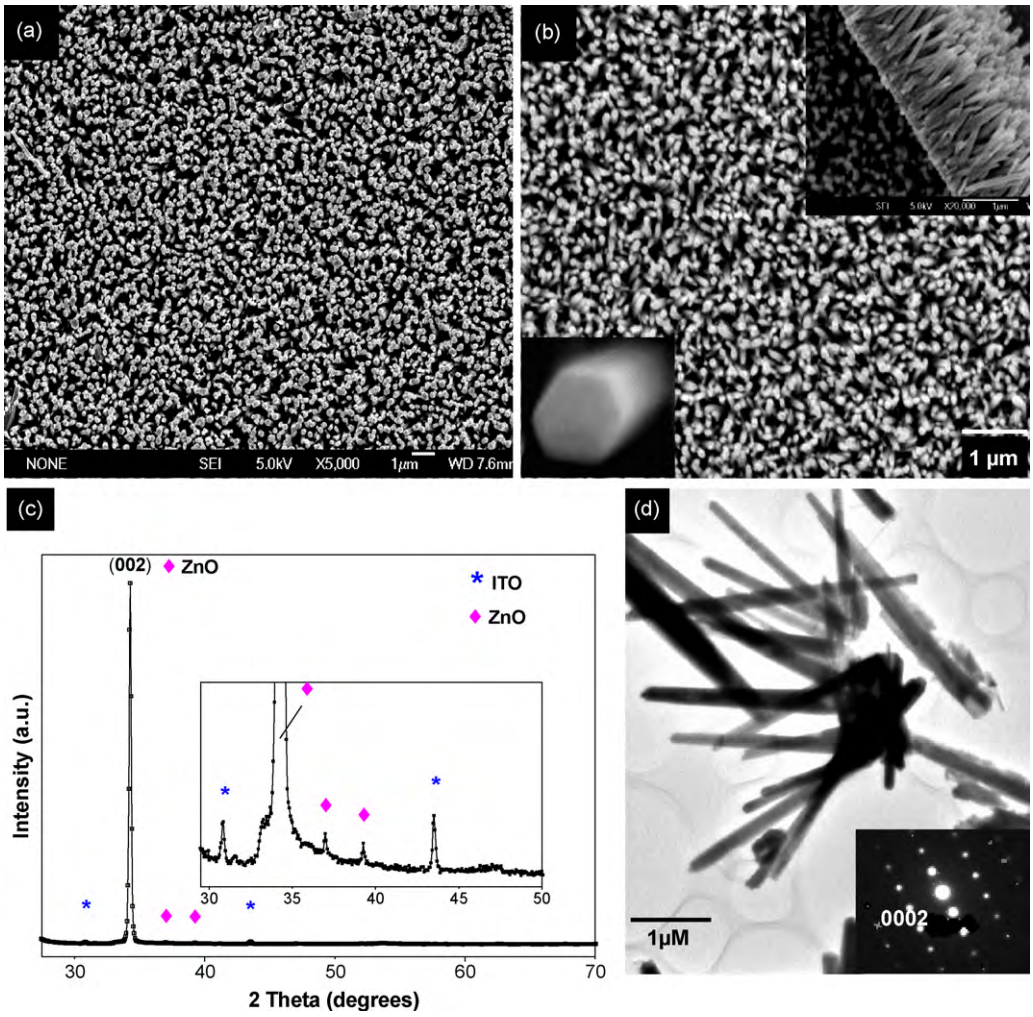

Fig. 2. (a, b) SEM images of hexagonal ZnO NRs. Inserts in Part (b) are the cross-sectional enlarged images. XRD (c) and TEM (d) images of hexagonal ZnO NRs. Insert in Part (d) is the SAED patterns.

are vertically aligned on the substrate. The hexagonal morphology and crystallization along the *c*-axis direction of ZnO NRs were reported elsewhere [6]. All the peaks can be readily indexed to hexagonal wurtzite ZnO (JCPDS Card No. 36-1451; space group $P6_3mc$, $a = 3.24982$ Å, $c = 5.20661$ Å) except for those arising from the IPS (see the enlarged image of the pattern in the insert). In the XRD pattern, the (0 0 2) peak is dominant, and its intensity is much higher than others, revealing the high *c*-axis growth orientation of the product. Further structural characterization of ZnO NRs was performed by TEM and SAED. Fig. 2d displays a TEM image of several individual ZnO nanorods. The SAED pattern taken from one of the rods (see the red cycle section) is shown in the insert.

3.3. Study of adhesion-controlled

We paid more attention to research on fabrication of the ZnO NRs with optimum density, stability and adhesion to substrate, and to explore a kind of ZnO NRs with optimal density (for better electron transmission capability) and OSR (for superior absorption capability to viologen molecules) to obtain excellent EC performance. The adhesion property of the ZnO NRs to IPS was investigated at first. After 120 times about 150 bending and 25 min ultrasonicating using 250 W and 40 Hz experiment, the SEM morphology images (including corresponding cross-section images) are shown in Fig. 3b and d originating from those in Fig. 3a and c, respectively. We can obviously find that the majority of the ZnO NRs using spinning-prepared seeds had been detached from the seed layer and the IPS, and many nanorods were, owing to bending and ultrasonicating process, broken to small parts from the NRs, as shown in Fig. 3d. In comparison, there were, as for the ZnO NRs grown using sputtering-prepared seeds, few nanorods detached from the seed layer and the IPS even though some were broken to small parts (see the SEM morphology images including corresponding cross-section images in Fig. 3b). So we can draw a conclusion that the ZnO NRs using sputtering-prepared seed layers shows superior adhesion property to substrate and resistance capacity to ultrasonicating and bending when compared with the spin-coated method.

3.4. Study of density-controlled, OSR and viologen-modified

Then the parameters of different densities and OSRs are listed in Table 1, and the effect of exploring their morphology, OSR, and absorption capability to viologen molecules is shown in Fig. 4. From Table 1, it can be found that the OSR depends on the nanorods' diameter and length and the density of NRs, especially the diameter and density, such as the huge different OSRs of Sample A with Low OSR (OSR, 26%, as shown in Fig. 4a) and Sample C with High OSR (OSR, 75%, as shown in Fig. 4c) results from their different diameters (Sample A, 132 nm; Sample C, 220 nm) though they have approximate density (Sample A, 1.90×10^9 rods cm^{-2}; Sample C, 1.60×10^9 rods cm^{-2}). Moreover, we can clearly observe that Fig. 4e, pristine ZnO NRs of which are shown in Fig. 4b,

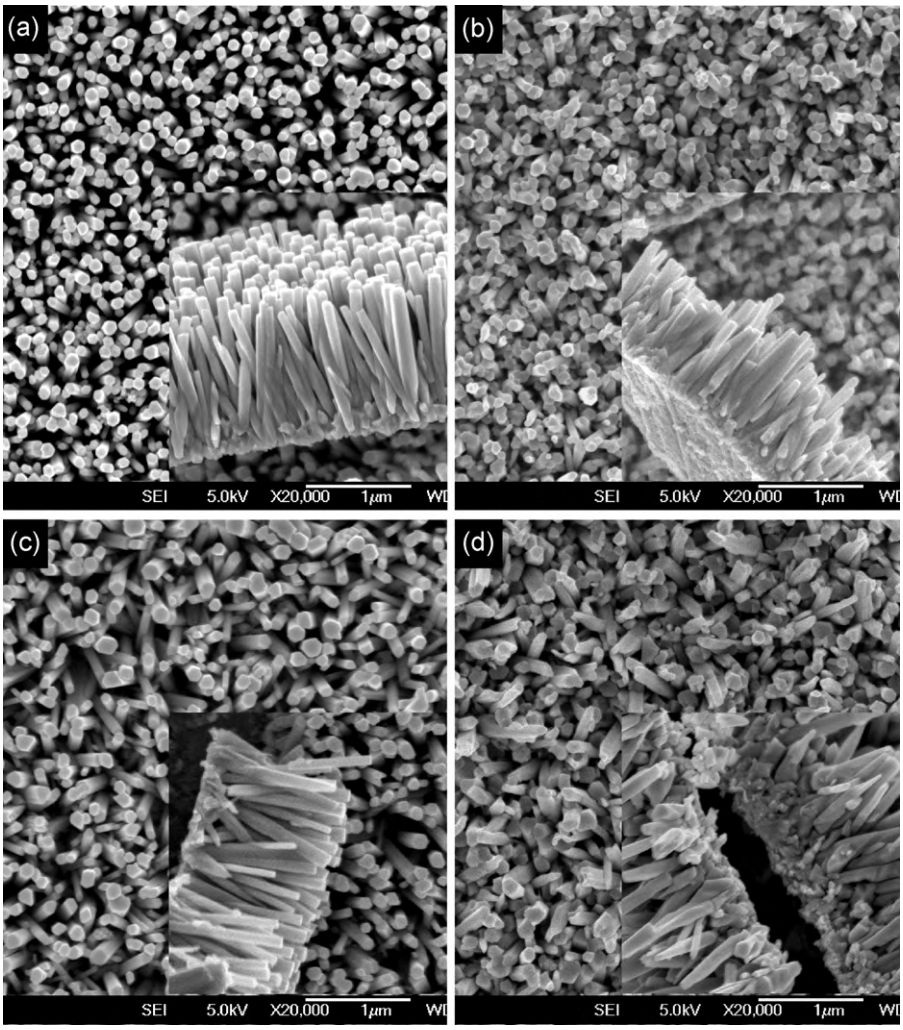

Fig. 3. (a, c) SEM images of the ZnO NRs pre-preparated ZnO seed layers using sputtering and spinning method, respectively. (b, d) SEM images of the (a) and (c) bended 120 times and ultrasonicated 25 min, inserts are the cross-sectional images of their respective arrays.

illustrates much more dominant absorption performance to viologen molecules than Fig. 4d and f, while their pristine ZnO NRs are shown in Fig. 4a and c, respectively. According to the OSR shown in Fig. 4a–c, we can come to a conclusion that the ZnO NRs of Low OSR (like Fig. 4a) and High OSR (like Fig. 4c) both go against absorption to viologen molecules compared with Opti-den OSR shown in Fig. 4b. Otherwise, we call Sample A Opti-den OSR (optimum OSR with apropos density) for not only it has the best absorption capability to viologen molecules but also ZnO NRs with apropos density (e.g., 3.34×10^9 rods cm^{-2}) can bring forth higher *c*-axis growth orientation and better electron transmission capability.

From the relevant kinetics conditions of ZnO NRs fabrication, it was also found that the NRs density could be primarily controlled by changing the thickness of the seed layer (except too thickness of the seed layer can result in polymer of many seeds so that NRs turn into sparse ones, e.g., Sample C and Fig. 4c), besides the nanorods' dimensions could be primarily dependent on the concentration and ratio of the reactants, the time and temperature of NRs growth. The experimental result shows that Opti-den OSR NRs with optimum density and OSR was fabricated in a 300 mL of aqueous solution containing 0.05 M $Zn(NO_3)_2{\cdot}6H_2O$ and 0.06 M $C_6H_{12}N_4$ at 75 °C for 24 h, and the sputtering time of ZnO seed layers was 80 s, as shown in Table 1 and Fig. 4b. At the same time, by changing the sputtering times for 40 s and 150 s, we obtained the ZnO NRs of Low OSR and High OSR, as shown in Fig. 4a and c, respectively. The latter higher OSR was mainly resulting from nanorods' too big dimension especially too big diameter though it has approximate density compared with the former (the former, $\sim 1.90 \times 10^9$ rods cm^{-2}; the latter, $\sim 1.60 \times 10^9$ rods cm^{-2}), and the temperature, time and concentration of growing High OSR ZnO NRs were adjusted at 95 °C for 30 h in a aqueous solution containing 0.06 M $Zn(NO_3)_2{\cdot}6H_2O$ and 0.08 M $C_6H_{12}N_4$. As a result, it is found that the diameter, density and OSR of the Opti-den OSR NRs are ~140 nm, $\sim 3.34 \times 10^9$ rods cm^{-2} and ~52%, respectively.

Table 1
Values of the ZnO NRs dimensions, density and OSR for different seed sputtering time.

Sample	Sputtering time (s)	Diameter (nm)	Length (μm)	Density ($\times 10^9$ rods cm^{-2})	OSR (%)
A: Low OSR (Fig. 4a)	40	132	1.41	1.90	26
B: Opti-den OSR (Fig. 4b)	75	140	1.41	3.34	52
C: High OSR (Fig. 4c)	150	220	2.10	1.60	75

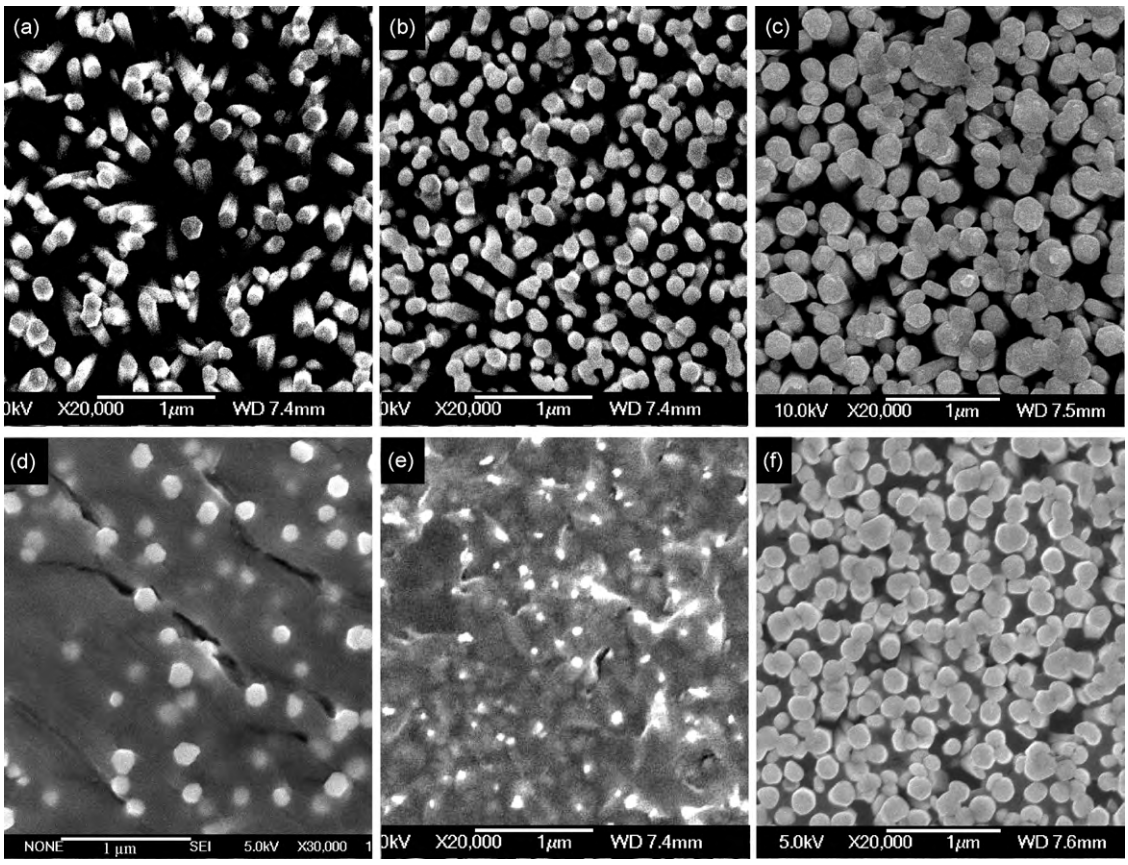

Fig. 4. (a–c) SEM images of different OSR ZnO NRs. (d–f) SEM images of different OSR ZnO NRs modified by 0.02 M methyl viologen solution for 72 h.

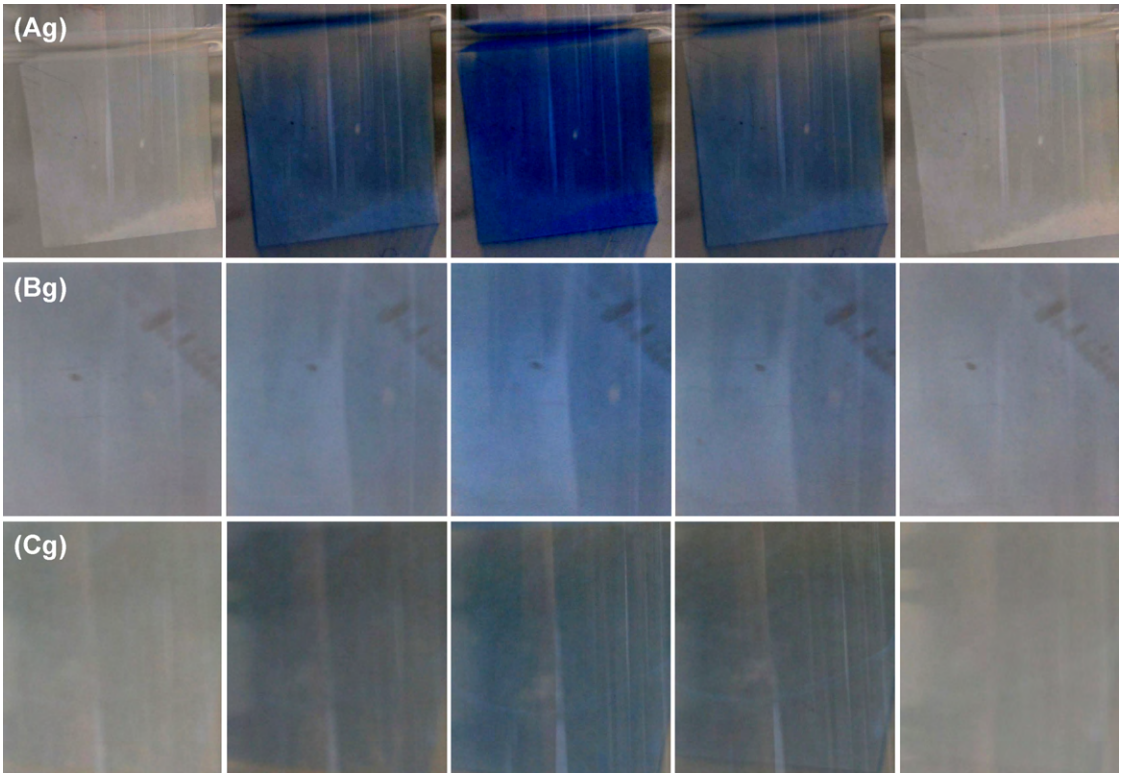

Fig. 5. EC performance photographs of the ZnO NRs with different OSRs: (Ag) Opti-den OSR; (Bg) Low OSR; and (Cg) High OSR.

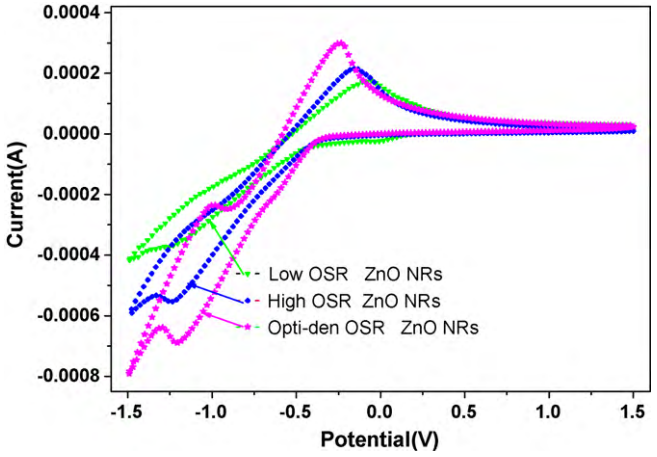

Fig. 6. Comparisons of the cyclic voltammograms (CVs) for High OSR, Low OSR and Opti-den OSR VMZs electrodes, respectively. The scan speed is 0.05 V/s.

3.5. Study of EC performance

Finally, in accordance with results of the EC performance of the different OSR ZnO NRs were also confirmed and shown in Figs. 5 and 6. As for the EC performance shown in Fig. 5, it is clearly found that the working electrode assembled using the VMZs with Opti-den OSR (optimum density and OSR, e.g., Fig. 5Ag) demonstrates better EC performance than the other two (Bg, Low OSR; Cg, High OSR). At the same time, Fig. 6 shows that the cyclic voltammograms curves were obtained with a 0.05 V/s scan speed for the three kinds of VMZs working electrodes: High OSR, Low OSR and Opti-den OSR, as shown respectively in Fig. 4f, d and e. From Fig. 6, we can find out that there are redox peaks for both the Low OSR and High OSR ZnO NRs electrodes, with the former ones bigger than the later ones. Otherwise, four obvious redox peaks are clearly found for the electrode of Opti-den OSR ZnO NRs. The two peaks located at −0.61 V and −1.21 V (vs Ag/AgCl sat. KCl reference electrode) during the reduction scan can be defined as the reductions that provide the singly and doubly reduced viologen species, when the two other peaks located at −1.00 V and −0.24 V are related to the oxidations of the singly and doubly reduced viologen, respectively [11]. The VMZs electrode is colored to blue during the reduction scan and bleached to transparency during the oxidation scan. The effect of the CVs curves is in accordance with that in Fig. 5.

4. Conclusion

In summary, our work presented here shows that growth ZnO NRs with different adhesions and densities could be controlled by adjusting the preparation method and thickness of ZnO seed layers. The ZnO NRs with optimum density and OSR (diameter, ~ 140 nm; density, ~3.34×10^9 rods cm^{-2}; and OSR, ~52%) can be obtained by using the solution containing 0.05 M $Zn(NO_3)_2{\cdot}6H_2O$ and 0.06 M $C_6H_{12}N_4$ at 75 °C for 24 h, before about 4–5 nm thickness of ZnO seed layers were sputtered. Moreover, the sputtering-coated ZnO NRs show superior adhesion property to substrate and resistance capacity to ultrasonicating and bending when compared with the spin-coated method. And it is found that the ZnO NRs with the optimum density and OSR demonstrate superior absorption capability to viologen molecules and excellent EC performance. Our results would provide a promising route to study flexible ECs and further find the optimized electrode structure.

Acknowledgement

We gratefully acknowledge financial support from the National Natural Science Foundation of China (Nos. 50872039; 50802032).

References

[1] M.H. Huang, S. Mao, H. Feick, H.Q. Yan, Y.Y. Wu, H. Kind, E. Weber, R. Russo, P.D. Yang, Science 292 (2001) 1897–1899.
[2] X.W. Sun, J.Z. Huang, J.X. Wang, Z. Xu, Nano Lett. 8 (2008) 1219–1223.
[3] X.D. Bai, E.G. Wang, P.X. Gao, Z.L. Wang, Nano Lett. 3 (2003) 1147–1150.
[4] X.D. Wang, J. Zhou, C.S. Lao, J.H. Song, N.S. Xu, Z.L. Wang, Adv. Mater. 19 (2007) 1627–1631.
[5] L. Chen, Y.S. Di, W. Lei, Q. Yin, X.B. Zhang, Z.W. Zhao, J. Phys. Chem. C 112 (2008) 13447–13449.
[6] J.P. Liu, X.T. Huang, Y.Y. Li, X.X. Ji, Z.K. Li, X. He, F.L. Sun, J. Phys. Chem. C 111 (2007) 4990–4997.
[7] S.J. Lim, S.J. Kwon, H. Kim, J.S. Park, Appl. Phys. Lett. 91 (2007), 183517-1–183517-3.
[8] M. Law, L.E. Greene, J.C. Johnson, R. Saykally, P.D. Yang, Nat. Mater. 4 (2005) 455–459.
[9] Z.L. Wang, J.H. Song, Science 312 (2006) 242–246.
[10] X.D. Wang, J.H. Song, J. Liu, Z.L. Wang, Science 316 (2007) 102–105.
[11] X.W. Sun, J.X. Wang, Nano Lett. 8 (2008) 1884–1889.
[12] C. Ma, M. Taya, C.Y. Xu, Electrochim. Acta 54 (2008) 598–605.
[13] S. Tarkuc, E. Sahmetlioglu, C. Tanyeli, I.M. Akhmedov, L. Toppare, J. Opt. Mater. 30 (2008) 1489–1494.
[14] C.Y. Jiang, X.W. Sun, K.W. Tan, G.Q. Lo, A.K.K. Kyaw, D.L. Kwong, Appl. Phys. Lett. 92 (2008), 143101-1–143101-3.
[15] J.P. Liu, Y.Y. Li, R.M. Ding, J. Jiang, Y.Y. Hu, X.X. Ji, Q.B. Chi, Z.H. Zhu, X.T. Huang, J. Phys. Chem. C 113 (2009) 5336–5339.
[16] H.C. Ko, S.A. Park, H.S. Lee, Synth. Met. 143 (2004) 31–35.
[17] S. Cho, S. Kim, N.H. Kim, U.J. Lee, S.H. Jung, E. Oh, K.H. Lee, J. Phys. Chem. C 112 (2008) 17760–17763.
[18] S. Xu, Y. Ding, Y.G. Wei, H. Fang, Y. Shen, A.K. Sood, D.L. Polla, Z.L. Wang, J. Am. Chem. Soc. 131 (2009) 6670–6671.
[19] C. Pacholski, A. Kornowski, H. Weller, Angew. Chem. Int. Ed. 41 (2002) 1188–1191.
[20] L. Vayssieres, K. Keis, S.E. Lindquist, A. Hagfeldt, J. Phys. Chem. B 105 (2001) 3350–3352.
[21] L. Vayssieres, Adv. Mater. 15 (2003) 464–466.
[22] J.X. Wang, X.W. Sun, Y. Yang, H. Huang, Y.C. Lee, O.K. Tan, L. Vayssieres, Nanotechnology 17 (2006) 4995–4998.
[23] L.E. Greene, M. Law, J. Goldberger, F. Kim, J.C. Johnson, Y.F. Zhang, R.J. Saykally, P.D. Yang, Angew. Chem. Int. Ed. 42 (2003) 3031–3034.